Global Biogeochemical Cycles

RESEARCH ARTICLE
10.1029/2024GB008176

Organic Coatings Reduce Dissolution Rate by an Order of Magnitude for Carbonate Minerals Produced by Marine Fish

Amanda M. Oehlert[1], Sarah Walls[2], Katelyn Arista[1], Jazmin Garza[1], Erik J. Folkerts[2], Brooke E. Vitek[1], Sadegh Tale Masoule[3], Clément G. L. Pollier[1], Gaëlle Duchâtellier[1], John D. Stieglitz[2], Daniel D. Benetti[2], Rachael M. Heuer[2], Ali Ghahremaninezhad[3], and Martin Grosell[2]

[1]Department of Marine Geosciences, Rosenstiel School of Marine, Atmospheric, and Earth Science, University of Miami, Miami, FL, USA, [2]Department of Marine Biology and Ecology, Rosenstiel School of Marine, Atmospheric, and Earth Science, University of Miami, Miami, FL, USA, [3]Department of Civil, Architectural, and Environmental Engineering, University of Miami, Miami, FL, USA

Abstract Marine carbonate production and dissolution are important components of the global carbon cycle and the marine alkalinity budget. Global carbonate production by marine fish (ichthyocarbonate) has been estimated to be as high as 9.03 Pg $CaCO_3$ yr^{-1}; however, the fate of ichthyocarbonate is poorly understood. High magnesium concentrations in ichthyocarbonate would traditionally suggest rapid dissolution under current marine conditions, but a correlation between dissolution rate and mol%$MgCO_3$ has not been observed. Here, we aim to determine the role of organic coatings on dissolution rates of ichthyocarbonate in marine environments. We applied a combination of petrographic, geochemical, and microCT approaches to assess the quantity and distribution of organic matter in ichthyocarbonate produced by two species of marine fish, the Gulf toadfish (*Opsanus beta*) and the Olive flounder (*Paralichthys olivaceus*). We show that organic matter, including external coatings and embedded organic material, is volumetrically significant, ranging from 8.5% to 32.3% of ichthyocarbonate by volume. Bleach oxidation of external organic matter coatings increased the dissolution rate of ichthyocarbonate by more than an order of magnitude, suggesting these coatings serve to reduce reactive surface area of the mineral fraction in ichthyocarbonate. Assuming that organic coatings do not influence sinking rates, external coatings extend the depth of ichthyocarbonate persistence in the water column by ~12–15×. Therefore, organic coatings are an important determinant of the role of ichthyocarbonate in the marine carbon cycle.

Key Points:

- Ichthyocarbonate-associated organic matter occurs as embedded material and exterior coatings
- Exterior organic matter coatings on ichthyocarbonate slow mineral dissolution by 12–15×
- Organic matter exerts an important control on ichthyocarbonate fate, and thus may determine the role of marine fish in the carbon cycle

Supporting Information:

Supporting Information may be found in the online version of this article.

Correspondence to:

A. M. Oehlert,
aoehlert@miami.edu

Citation:

Oehlert, A. M., Walls, S., Arista, K., Garza, J., Folkerts, E. J., Vitek, B. E., et al. (2024). Organic coatings reduce dissolution rate by an order of magnitude for carbonate minerals produced by marine fish. *Global Biogeochemical Cycles*, *38*, e2024GB008176. https://doi.org/10.1029/2024GB008176

Received 18 MAR 2024
Accepted 4 OCT 2024

Author Contributions:

Conceptualization: Amanda M. Oehlert, Rachael M. Heuer, Martin Grosell
Formal analysis: Amanda M. Oehlert, Sarah Walls, Katelyn Arista, Jazmin Garza, Erik J. Folkerts, Brooke E. Vitek, Sadegh Tale Masoule, Clément G. L. Pollier, Gaëlle Duchâtellier, Rachael M. Heuer, Martin Grosell
Methodology: Amanda M. Oehlert, Erik J. Folkerts, Sadegh Tale Masoule, Clément G. L. Pollier, Rachael M. Heuer, Ali Ghahremaninezhad, Martin Grosell
Resources: Amanda M. Oehlert, Daniel D. Benetti, Ali Ghahremaninezhad

1. Introduction

Changes in the magnitude, rate, and composition of carbon fluxes to the deep ocean exert tremendous impact on Earth's climate (Sarmiento et al., 1998), the distribution of oxygen and nutrients (DeVries & Weber, 2017), and marine ecosystem productivity (Broecker & Peng, 1982; Ducklow et al., 2001) through geological time. Recent studies have recognized the significant role of particulate carbonate produced by marine bony fish (ichthyocarbonate) in both the global carbon cycle and marine alkalinity budgets (Folkerts et al., 2024; Ghilardi et al., 2023; Oehlert, Garza, et al., 2024; Saba et al., 2021; Wilson et al., 2009; Woosley et al., 2012). However, significant knowledge gaps surrounding ichthyocarbonate production magnitude and fate currently preclude their integration into fully coupled Earth system models and our understanding of their role in global carbon cycling (Saba et al., 2021). Here, we address the unknown role of the organic coating associated with ichthyocarbonates on their fate in oceanic environments. Initial work by Wilson et al. (2009), assuming a global fish biomass of ~0.9–2.1 Gt, indicated that marine fish can conceivably be responsible for 3%–15% (0.33–0.93 Pg $CaCO_3$ yr^{-1}), but potentially as much as 45% of annual carbonate production in the oceans. Since then, technological advances have resulted in significantly larger global fish biomass estimates, ranging between 2.0 and 19.5 Gt (Bar-On et al., 2018; Bianchi et al., 2021; Irigoien et al., 2014; Jennings & Collingridge, 2015; Proud et al., 2017, 2018, 2019), suggesting a much higher global production of ichthyocarbonate than initially estimated. Linearly extrapolating global ichthyocarbonate production by more recent estimates of global fish biomass suggests that the global ichthyocarbonate production rate can range from 0.33 to 9.03 Pg $CaCO_3$ yr^{-1} (Oehlert, Garza, et al., 2024). Despite the growing appreciation for the important role of ichthyocarbonate production in the global carbon cycle, only a few studies have investigated the fate of excreted ichthyocarbonate, especially as it applies in

Visualization: Amanda M. Oehlert, Katelyn Arista, Brooke E. Vitek, Sadegh Tale Masoule, Martin Grosell
Writing – original draft: Amanda M. Oehlert, Sadegh Tale Masoule
Writing – review & editing: Amanda M. Oehlert, Sarah Walls, Katelyn Arista, Jazmin Garza, Erik J. Folkerts, Brooke E. Vitek, Sadegh Tale Masoule, Clément G. L. Pollier, Gaëlle Duchâtellier, Daniel D. Benetti, Rachael M. Heuer, Ali Ghahremaninezhad, Martin Grosell

the open ocean (Folkerts et al., 2024; Foran et al., 2013; Woosley et al., 2012). Without robust and empirical observations of the ichthyocarbonate dissolution rate, predictions regarding the impact of marine fish on global alkalinity budgets and the carbon cycle are limited (Dunne et al., 2012; Saba et al., 2021; Subhas et al., 2022).

Ichthyocarbonate produced by the Gulf toadfish (*Opsanus beta*) (Woosley et al., 2012) and the Gilthead Seabream (*Sparus aurata*) (Foran et al., 2013) were found to have ∼1.95× higher solubility than aragonite in filtered seawater at 25°C in both studies. Based on these observations, Woosley et al. (2012) suggested that dissolution of ichthyocarbonate may be responsible for excess normalized total alkalinity concentrations above the aragonite saturation horizon, although conflicting conclusions were presented by a recent study of carbonate chemistry in the North Pacific (Subhas et al., 2022). Relatively high solubility of ichthyocarbonate has largely been proposed to result from high mol%$MgCO_3$ in ichthyocarbonate (Walsh et al., 1991; Wilson et al., 2009; Woosley et al., 2012). Mineralogical analyses showed that high-magnesium calcite (HMC) and amorphous calcium magnesium carbonate phases ("ACMC," Foran et al., 2013; Perry et al., 2011; Salter et al., 2012, 2014, 2017, 2018) dominate the carbonate components in ichthyocarbonate. Prior studies of other forms of biogenic HMC have reported increasing mineral solubility with increasing mol%$MgCO_3$ (Bischoff et al., 1987; Chave et al., 1962; Morse & Mackenzie, 1990), compatible with the hypothesis that the high mol%$MgCO_3$ of ichthyocarbonate is likely to drive high dissolution rates (Foran et al., 2013; Perry et al., 2011; Salter et al., 2012, 2014, 2017, 2018; Woosley et al., 2012). However, a recent study of dissolution rates of ichthyocarbonate produced by three marine fish species conducted across a range of aragonite saturation indicated heterogeneous dissolution rates unrelated to mol%$MgCO_3$ (Folkerts et al., 2024). Thus, alternative controls on the ichthyocarbonate dissolution rate, such as organic matter coatings and the presence of microbial communities, were hypothesized to play more important roles in the fate of ichthyocarbonate (Folkerts et al., 2024; Grosell & Oehlert, 2023).

Organic matter has previously been linked to both enhanced (Archer, 1991; Emerson & Bender, 1981; Milliman et al., 1999) and depressed (Honjo & Erez, 1978; Keir, 1980) dissolution rates in sinking carbonate particles. Enhanced dissolution rates were proposed to be associated with microbial degradation of the associated organic matter, which has been hypothesized to lead to localized increases in CO_2 (Godoi et al., 2009; Milliman et al., 1999). On the other hand, dissolution rates of biogenic carbonates treated with bleach to oxidize organic coatings were elevated relative to non-bleached biogenic carbonate minerals produced by foraminifera, bivalves, as well as synthetic and spar calcite, leading investigators to propose that organic coatings reduce the reactive surface area of sinking particles and depress dissolution rates (Berger, 1967; Corliss & Honjo, 1981; Glover & Kidwell, 1993; Honjo & Erez, 1978; Naviaux, Subhas, Dong, et al., 2019; Oelkers et al., 2011; Suess, 1970). Subhas et al. (2019) differentiated between surface coatings of organic matter and those incorporated within the coccolith lattice. Coatings were not found to induce significant dissolution rate differences; however, intracrystalline organic matter in the lattice was hypothesized to promote re-precipitation or even suppress dissolution rates (Subhas et al., 2019). Although insightful, these prior studies focused on biogenic carbonates characterized by low magnesium calcite, aragonite, or high magnesium calcite with mol%$MgCO_3$ significantly lower than that observed in ichthyocarbonate (Foran et al., 2013; Perry et al., 2011; Salter et al., 2012, 2017, 2018, 2019). Furthermore, ichthyocarbonate is known to contain significant quantities of organic matter (∼5–40% d.w.; Oehlert, Garza, et al., 2024), but the composition of this organic matter has yet to be described. For instance, it remains unknown whether organic matter is similar in ichthyocarbonate produced by different species of fish, and whether intestinal microbial communities (i.e., Walsh et al., 1991) significantly contribute organic matter to ichthyocarbonate.

Here, we specifically addressed knowledge gaps about the origin of ichthyocarbonate organic matter and the impact of organic matter coatings on ichthyocarbonate dissolution rates. To accomplish this, we evaluated the composition, quantity, and spatial distribution of organic matter in ichthyocarbonate, and assessed whether organic matter coatings enhance or reduce the dissolution rates of ichthyocarbonate produced by two species of marine fish. Measurements of C/N ratios and $\delta^{13}C_{org}$ values were used to assess whether the compositional characteristics of organic matter in ichthyocarbonate could be attributed to fish or microbial sources. To determine the role of organic coatings on the dissolution rate of ichthyocarbonate, we compared the dissolution rates of ichthyocarbonate with intact organic matter coatings to those where the organic coating was degraded with bleach. We show here that the quantity and distribution of organic matter significantly impacts the dissolution rate, and thus the ultimate fate, of ichthyocarbonate. Results indicate that organic matter coatings play an important role in extending the depth to which sinking ichthyocarbonate persists in the oceans.

2. Materials and Methods

2.1. Ichthyocarbonate Collection

Samples of ichthyocarbonate were collected as previously (Folkerts et al., 2024; Oehlert, Garza, et al., 2024; Salter et al., 2018, 2019), using disposable pipettes, from the bottoms of tanks holding *O. beta* (Gulf toadfish) and *Paralichthys olivaceus* (Olive flounder) in the Environmental Physiology and Toxicology laboratory or from the University of Miami's Experimental Hatchery (UMEH) at the Rosenstiel School under Institutional Animal Care and Use Committee (IACUC) protocols No. 19–201 and 20–138. Magnesium concentrations were determined previously with Olive flounder icthyocarbonate containing 24.5 mol%$MgCO_3$ and Gulf toadfish ichthyocarbonate containing 32.3% (Folkerts et al., 2024). Upon collection, samples of ichthyocarbonate were treated differently depending on the analytical procedure for which they were destined, the details of which are described in the following sections.

2.2. Wet Thin Sections

Wet thin sections of ichthyocarbonate produced by the two species were prepared to facilitate examination of the spatial relationships between organic matter and minerals. Ichthyocarbonate samples destined for wet thin section preparation were preserved in a 3.7% (v/v) solution of formalin and filtered seawater and stored in a refrigerator at 4°C. Wet thin section preparation techniques were developed by Nye et al. (1972) to preserve the three-dimensional relationship of the organic components in the system with the minerals by maintaining sample hydration through the embedding process (Vitek et al., 2022). The resulting samples were mounted on glass microscope slides, cut, and polished to approximately 20 μm thickness using conventional thin sectioning techniques on a Hillquist thin section machine, and subsequently stained with crystal violet as previously described (Vitek et al., 2022) to identify cell membranes and negatively charged biomass. An Olympus BH-2 petrographic microscope equipped with plane-polarized and cross-polarized transmitted light was used to examine thin sections; photomicrographs were collected using a Lumenera Infinity 3 digital microscope camera (Infinity Analyze v 6.5.6) as previously described (Vitek et al., 2022).

2.3. X-Ray Microcomputed Tomography (Micro-CT)

Micro-CT analyses were conducted to assess the volume of organic matter in ichthyocarbonate for comparison with dry weight measurements published previously. Ichthyocarbonates were collected in 0.2 mL PCR tubes and filled with UV-sterilized and 0.22 μm filtered seawater from Biscayne Bay to cover the precipitates. PCR tubes were scanned with a Bruker 1273 Skyscan micro-CT instrument within hours of collection. The pellets were irregularly shaped, and ranged from 0.25 to 2 mm in diameter, and larger ones were chosen for detailed analysis. The instrument has a Varex 2315 camera, which is a high speed, low noise X-ray detector capable of detecting features as small as a few μm with a pixel matrix of 3072 by 1944. The X-ray source was a Hamamatsu L9181-02 with an operation range of 40–130 kV and 10–130 μA. Due to the samples' low density and size, the scans were performed at 50 kV and 50 μA with no filters, at a pixel size of 6 μm, and an exposure time of 3,000 ms. Projections were taken at 0.4-degree intervals and averaged for 10 frames in each step. A total of 518 unique projections were collected.

The X-ray projections were then reconstructed with Bruker NRecon software. The scans did not need any post-scan adjustments, and parameters including smoothing, beam hardening, and ring artifact correction were set to zero. The dynamic range was set between 0 and 0.05. A total of 1,510 slices were reconstructed for each vial of precipitates. For the analysis, the boundary of 5 individual ichthyocarbonates per species were manually mapped every third slice and then saved into a new data set to be analyzed separately using CTan Analytical Suite. Based on visual sample characteristics of density, segmentation analyses were conducted for each grain. Organic matter in ichthyocarbonate produced by the Gulf Toadfish was delineated using thresholds of 50–100 in the grayscale index, while carbonate ranged from 110 to 255 on the grayscale index. Visual differences in ichthyocarbonate produced by the Olive Flounder resulted in thresholds for organic matter that started at the low end at 30, and a high threshold between 75 and 130 on the grayscale index. The carbonate was segmented as the residual up to 255.

2.4. Geochemical Analyses

Geochemical analyses of organic matter in ichthyocarbonate were conducted to determine whether compositional differences exist in ichthyocarbonate produced by different species. Samples destined for elemental and stable carbon isotope analyses were rinsed briefly three times in ultrapure (18 MΩ.cm) MilliQ water and dried in an oven at 35°C overnight. Dry samples were weighed and dissolved in 10% HCl, and the insoluble residue was collected by vacuum filtration using Whatman GF/C filters as previously described (Oehlert, Garza, et al., 2024; Oehlert & Swart, 2014; Oehlert et al., 2019). Filters were combusted using a Costech ECS4010 (Costech Analytical Technologies, Inc., Valencia, CA, USA) and the resulting CO_2 gas was transferred to a Delta V Advantage (Thermo Fisher Scientific, Waltham, MA, USA) for stable isotope measurement in the Stable Isotope Laboratory at the University of Miami. Reproducibility was ±0.1‰ as indicated by the standard deviation of replicate analyses of internal standards (n = 13) for $\delta^{13}C$ values of the organic matter. All data are reported relative to the Vienna Pee Dee Belemnite (V-PDB) scale, defined for organic carbon as the $\delta^{13}C$ value of graphite (USGS24) = −16.05‰ versus V-PDB (Coplen et al., 2006). C/N ratios measured by the Costech ECS 4010 are reported as molar ratios, and the standard deviation on the analysis was ±0.28.

2.5. Dissolution Rate

Dissolution rates were measured on untreated and bleach-treated ichthyocarbonate produced by the Gulf toadfish and the Olive flounder to determine whether organic matter coatings influence dissolution rates, and also to provide empirically constrained data for fate modeling described in Section 2.6. Ichthyocarbonate collected from both species was split into two subsamples. The first subsample received no pre-treatment prior to dissolution rate measurements, while the second subsample was leached for 90 min in a 50% solution of commercial bleach diluted (v/v) with filtered seawater at room temperature (measured pH = 10.7). Bleach was chosen to oxidize the organic matter because it has frequently been used in other studies of ichthyocarbonate to remove the mucus coating on ichthyocarbonate (Perry et al., 2011; Salter et al., 2012, 2014, 2017, 2018; Woosley et al., 2012), and it is characterized by high pH values (>10, Crowley & Wheatley, 2014; Honjo & Erez, 1978; Keir, 1980; Subhas et al., 2019) that are not likely to dissolve the carbonate in the sample. After the leaching period was complete, the supernatant was carefully removed with a pipette and discarded. The remaining solid material was rinsed briefly in seawater three times to remove any bleach residues, and the sample was immediately used in dissolution rate measurements alongside unbleached subsamples.

Digestion efficiency of the 50% bleach solution was assessed using a mixture of certified reference materials (CRM) including IAEA 413 and NCS DC70301 (Brammer Standard Geological Materials) in mass proportions approximating known ichthyocarbonate composition for the species investigated here (~95% carbonate, ~5% organic matter (Oehlert, Garza, et al., 2024)). Following the protocol described above, these mixtures of the CRMs were also treated with the 50% bleach solution for 90 min. The supernatant was carefully removed, the sample was rinsed three times in MilliQ water, and the residual was allowed to dry overnight in a Class 100 exhausted hood. Dry weights were collected and used to assess mass loss of the organic fraction only, since carbonates were assumed to be stable at alkaline pH values of commercial bleach. Digestion efficiency is reported as %mass loss. Scanning electron microscope imaging of bleach-treated ichthyocarbonate produced by the Gulf toadfish was conducted in order to compare to previously published images of natural ichthyocarbonate produced by the same species to confirm no change in crystallite morphology (and thus mol%$MgCO_3$, i.e., Salter et al., 2018) from bleach treatment. Detailed methods are provided in Supporting Information S1.

Measurement of the ichthyocarbonate dissolution rate was conducted as previously described (Folkerts et al., 2024). In brief, known weights of ichthyocarbonate samples were introduced into aeration tubes allowing for gentle agitation of ichthyocarbonate during the experimental period. Tubes were filled with 15 mL of ambient temperature, UV-sterilized and filtered seawater, and dissolution was allowed to proceed for measured periods of time ranging from 1.5 to 4 hr. Controls were conducted simultaneously by measuring changes in seawater with no ichthyocarbonate. After the dissolution period, 10 mL of the solution was removed, centrifuged for less than 30 s, and analyzed using double endpoint total titratable alkalinity measurements described previously (Brix et al., 2013). Rates of ichthyocarbonate dissolution were calculated as described previously (Folkerts et al., 2024) and expressed in μmol eqv g^{-1} hr^{-1}.

2.6. Modeling the Fate of Ichthyocarbonate With and Without Organic Matter Coatings

To determine whether differences in the dissolution rate driven by organic matter coatings exert a significant impact on the predicted depth of completed dissolution, we modeled the fate of ichthyocarbonate with and without organic matter coatings. To accomplish this, we used a recently published model based on Stoke's law for settling velocities that was specifically developed to estimate the depth of complete ichthyocarbonate dissolution (Folkerts et al., 2024). This modeling approach assumes spherically shaped particles with a seawater specific gravity of 1.030 g mL^{-1} at 20°C and incorporates the measured specific gravity of ichthyocarbonate produced by the Gulf toadfish and Olive flounder, which was characterized previously (Folkerts et al., 2024). In brief, sinking rates were calculated using the buoyant velocity integrated approach that integrates particle specific gravity and size, as previously reported (Zheng & Yapa, 2000). Then, using average measured dissolution rates for natural and bleach-treated ichthyocarbonate produced by both species, we calculated the fate of sinking particles using two diameters (0.36 and 0.91 mm) to model the fate ichthyocarbonate most likely to reach depths below the euphotic zone, as previously reported (Folkerts et al., 2024). These diameters were selected because ichthyocarbonates <0.36 mm (~50% of global production) were predicted to fully dissolve before reaching a water depth of 500 m when excretion is assumed to occur in the surface waters of the ocean (Folkerts et al., 2024). Particles with diameters greater than 0.91 mm (~25% of global production; Folkerts et al., 2024) were predicted to reach oceanic depths greater than 1,000 m, where millennial scale sequestration is thought to be achieved (Bianchi et al., 2021). Through this approach, both the measured dissolution rates as well as the diminishing size of ichthyocarbonate with depth occurring as a function of dissolution were used to estimate complete dissolution depths. Although fish biomass is heterogeneously distributed with depth, here we assume that all ichthyocarbonate excretion occurs at the surface of the ocean to maintain a comparable starting depth between calculations of fate for ichthyocarbonate produced by different fish species. While the influence of temperature on seawater viscosity is implicitly considered in this model (Folkerts et al., 2024), the influences of temperature, pressure, and aragonite saturation state on dissolution rates, which change with depth, were not considered in these estimates.

2.7. Statistical Tests

Two-tailed *t*-tests were used to compare the results of MicroCT and geochemical analyses between bleach treated and natural ichthyocarbonate. Mann Whitney U tests were used to investigate significant differences in dissolution rates between bleach-treated and natural ichthyocarbonate because of differences in data set lengths. In all instances, significant differences were defined when p values were less than 0.05.

3. Results

3.1. Wet Thin Sections

Petrographic characteristics of the ichthyocarbonate and distribution of the organic matter in the sample were identified via observation of the wet thin sections. Ichthyocarbonate pellets ranged in size from 0.5 to 2 mm for both species (Figures 1a and 2a). Organic components in the ichthyocarbonate were stained in shades of blue and purple by positively charged crystal violet. Wet thin section analysis of ichthyocarbonates produced by both species demonstrated the presence of a thick exterior coating of organic matter (Figures 1 and 2; see abundance and distribution of organic matter stained purple with crystal violet), as well as the presence of organic matter throughout the ichthyocarbonates, which occurred in various morphologies.

In plane polarized light, Gulf toadfish ichthyocarbonate appeared sometimes as single pellets ranging in size from ~1.0 to 2.8 mm, and are sometimes comprised of an aggregate of smaller pellets ranging in size from ~0.25 to 0.5 mm (Figures 1a–1d). Organic matter and putative microbial cells were frequently observed around the edges of the smaller pellets within the aggregated ichthyocarbonate grains (Figures 1a, 1c, and 1e). Within ichthyocarbonate grains, purple staining highlighted both diffuse organic matter (Figure 1a, red box), distinct organic matter components (Figure 1a, arrow), as well as microbial cells (Figure 1c). Under higher magnification, the diffuse organic matter distributed within the toadfish ichthyocarbonate pellets exhibited a dendritic network texture, as well as long linear ropey features (Figure 1e). Carbonate components in the ichthyocarbonate predominantly occurred as fine microcrystalline carbonate ("micrite") that varied in color across the samples (Figure 1a). Observation under cross polarized light (Figures 1b, 1d, and 1f) highlights the anisotropic crystalline phases characterized by high birefringence. Figures 1d and 1f show small, ellipsoid features scattered throughout the micrite matrix, characterized by strong birefringence.

10.1029/2024GB008176

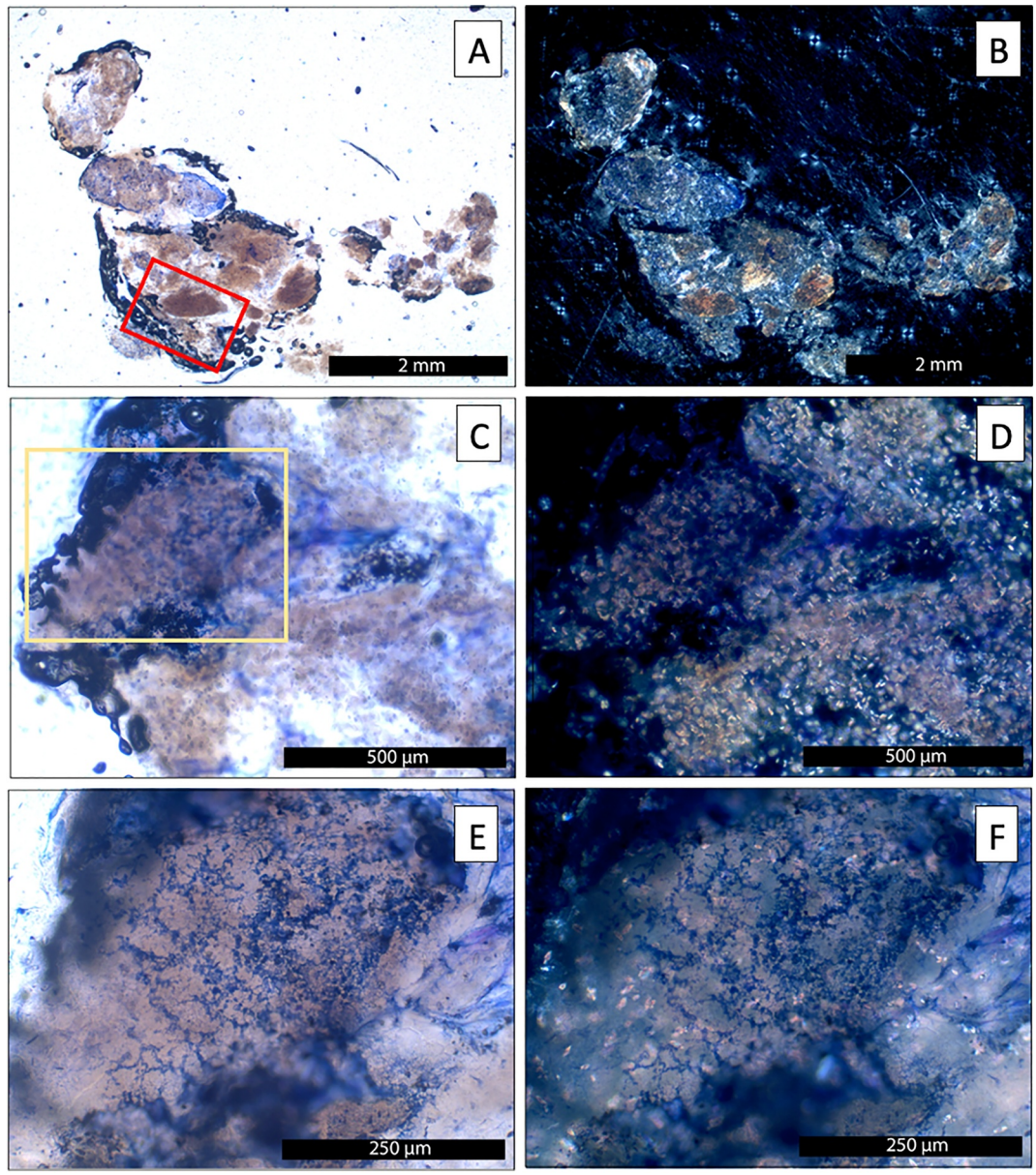

Figure 1. Photomicrographs of wet thin sections of ichthyocarbonate produced by the Gulf toadfish (*Opsanus beta*) stained with crystal violet in plane (a, c, e) and cross-polarized (b, d, f) light at increasing magnifications. Panel (c) shows area outlined in red box in (a), and (e) shows area outlined in yellow box in (c). Areas stained in shades of blue and purple are organic matter, while the carbonate precipitates occur in shades of brown. Note the thick mucus envelope in (a), (c), and (e), as well as the presence of organic material throughout the interior of the ichthyocarbonate pellet.

Ichthyocarbonate produced by the Olive flounder was also comprised of grains that appeared to be a single pellet ranging in size from ~0.9 to 2.5 mm, and also pellets that contained aggregates of multiple smaller grains ranging in size from ~0.6 to 1 mm (Figures 2a and 2b). Large pieces of organic matter that were stained purple were also observed in this species but lacked visual evidence of carbonate embedded within this component (Figure 2a, white arrow). Thick purple staining around the edges of most pellets and smaller composite grains was observed under plane polarized light. Within ichthyocarbonate pellets, composite grains were often bounded around the edges by organic matter (Figures 2a, 2c, and 2e), and densely packed clumps of organic matter were observed in one of the composite grains with unstained spherical areas approximately 10–50 µm in diameter embedded throughout (Figures 2a and 2c). With higher magnification, diffuse purple staining was observed throughout the ichthyocarbonate produced by the Olive Flounder. Pockets of coccoid-shaped microbial cells were observed in

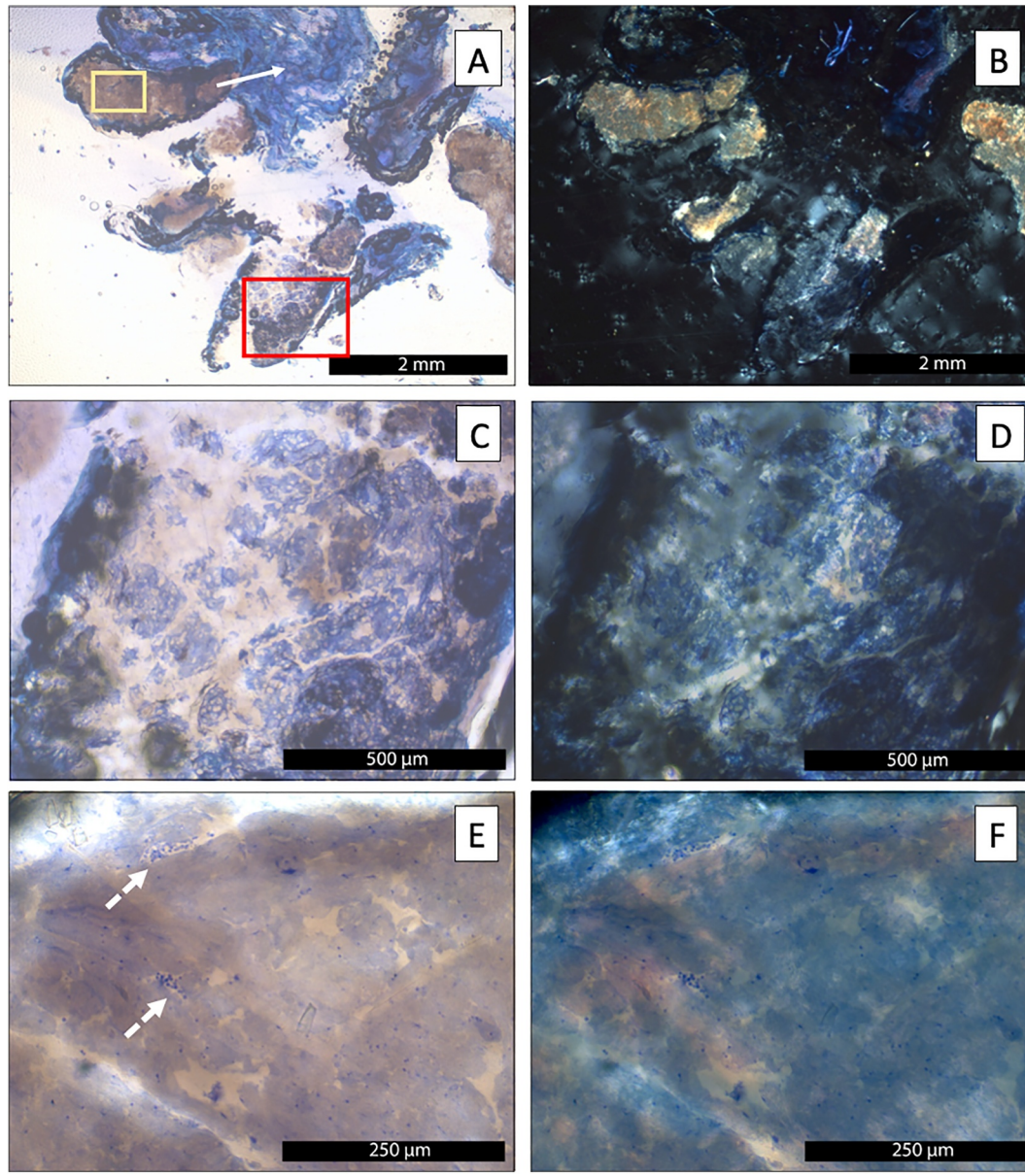

Figure 2. Photomicrographs of wet thin sections of ichthyocarbonate produced by the Olive flounder (*Paralichthys oliveaceus*) stained with crystal violet in plane (a, c, e) and cross-polarized (b, d, f) light at increasing magnifications. Panel (c) shows area outlined in red box in (a), and (e) shows area outlined in yellow box in (a). Areas stained in shades of blue and purple are organic matter, while the carbonate precipitates occur in shades of brown in plane polarized light. Note the extensive mucus (white arrow) in (a), as well as the presence of organic material throughout the interior of the ichthyocarbonate pellet (b, c). Clumps of organic matter containing apparent void spaces may reflect the presence of positively charged biomass (c), while small coccoid shaped bacteria with negatively charged biomass are visible in (e) (white dashed arrow).

between the diffusely stained organic matter (Figure 2e, white dashed arrows). Carbonate components in the ichthyocarbonate produced by the Olive flounder were characterized by more subdued birefringence under cross polarized light and lacked strongly birefringent ellipsoidal features (Figures 2d and 2f).

3.2. MicroCT Analysis

MicroCT analysis of five ichthyocarbonate particles per species revealed significant differences in the volumetric abundance of organic matter and carbonate in ichthyocarbonate produced by the Gulf toadfish and the Olive

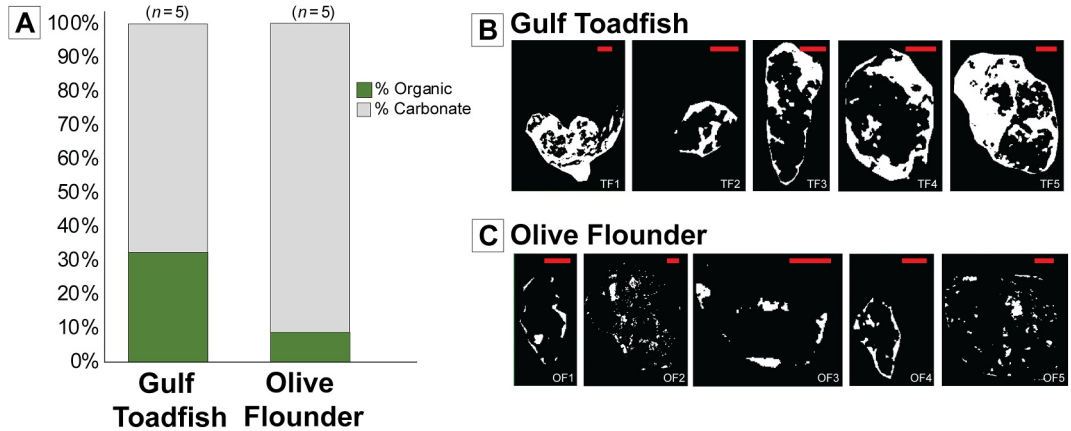

Figure 3. Results of MicroCT segmentation analysis. (a) Shows the average volumes of organic matter and carbonate minerals as segmented from five whole ichthyocarbonates produced by the Gulf Toadfish (b) and Olive flounder (c). Reconstructed cross sections from each of the five ichthyocarbonate particles mapped for both species are shown in (b) and (c). White areas show the distribution of organic matter, and red scale bars are all 250 μm.

flounder ($p < 0.01$). Ichthyocarbonate produced by the Gulf toadfish contains significantly more organic matter (32.3% ± 14.7%) than that produced by the Olive flounder (9.5% ± 3.9%, $p < 0.01$; Figure 3). Organic matter in ichthyocarbonate produced by the Olive Flounder has a lower degree of anisotropy (1.89 ± 0.24, $n = 5$) and pore thickness (0.03 ± 0.00 mm, $n = 5$) than that produced by the Gulf toadfish (2.24 ± 0.18 and 0.06 ± 0.00 mm, respectively, $n = 5$ for both data sets, $p < 0.05$ for both comparisons). Surface to volume ratios of organic matter were significantly higher in ichthyocarbonate produced by the Olive flounder (190 ± 24 1/mm) than the Gulf toadfish (92.6 ± 35.6 1/mm, $p < 0.01$). Ichthyocarbonate-associated organic matter produced by the Gulf toadfish was prevalent both within the interior of the particles as well as in exterior coatings (Figure 3b), while organic matter in ichthyocarbonate produced by the Olive Flounder is typically concentrated around the exterior of the particles (Figure 3c).

3.3. Geochemical Analyses

C/N ratios in bulk organic matter in ichthyocarbonate produced by the Gulf toadfish ranged from 6.48 to 9.94, and averaged 7.65 ± 1.61 ($n = 6$, Figure 4). The molar C/N ratio in organic matter of ichthyocarbonate produced by the Olive Flounder ranged from 6.55 to 8.68 and averaged 7.66 ± 0.81 ($n = 6$, Figure 4).

The average $\delta^{13}C_{org}$ value of the organic matter in ichthyocarbonate produced by Olive Flounder ($n = 6$) was −21.2 ± 0.02‰, lower than the average $\delta^{13}C_{org}$ value of ichthyocarbonate-associated organic matter produced by the Gulf toadfish (−19.3‰; Oehlert, Garza, et al., 2024). Two-tailed *t*-tests assessing variation in weight percent nitrogen, weight percent carbon, and average $\delta^{13}C_{org}$ values indicated a significant difference ($p < 0.05$) between organic matter associated with ichthyocarbonate produced by the Gulf toadfish ($n = 6$) and Olive flounder ($n = 6$). No significant differences were observed between species for C/N ratios ($p > 0.05$).

3.4. Dissolution Rate

Experiments assessing organic matter mass loss after leaching in the 50% bleach solution using mixtures of certified reference materials were conducted in triplicate and revealed that 59.2 ± 20.7% ($n = 3$) of the organic matter was oxidized during this treatment process. Comparison of bleach-treated ichthyocarbonate produced by the Gulf toadfish to natural ichthyocarbonate using Scanning Electron Microscopy revealed consistent crystallite morphology between treatments (Figures S1 and S2 in Supporting Information S1).

Dissolution rates measured for untreated ichthyocarbonate produced by the Gulf toadfish and Olive Flounder (Figure 5) were ~32 and 20 μeqv g^{-1} hr^{-1}, respectively, which agree with previous observations for these species (Folkerts et al., 2024). Subsamples treated with 50% bleach solution (Figure 5) dissolved 15 and 13 times faster than unbleached controls for Gulf toadfish and Olive flounder ichthyocarbonate, respectively. No significant difference was observed in the dissolution rates of natural ichthyocarbonate produced by the Gulf toadfish and the

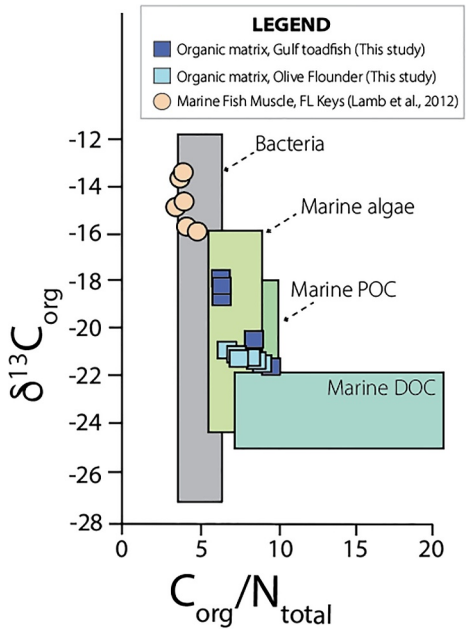

Figure 4. Cross plot of the molar ratio of organic carbon to total nitrogen content (C/N) versus the $\delta^{13}C_{org}$ value of the organic matter embedded in ichthyocarbonate produced by the Gulf toadfish (*Opsanus beta*; blue squares, *this study*), the Olive Flounder (*Paralichthys olivaceus*; aqua squares, *this study*), and marine fish muscle from the Florida Keys (orange circles; data from Lamb et al. (2012)). Shaded polygons in the background show ranges of $\delta^{13}C_{org}$ and C/N for organic matter sources in coastal waters published previously (Lamb et al., 2006). POC = particulate organic carbon, DOC = dissolved organic carbon.

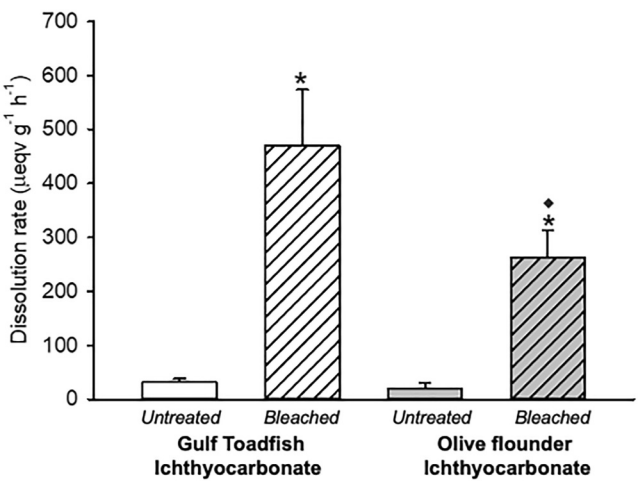

Figure 5. Comparison of average dissolution rates for bleached (hatched bars) and untreated (open bars) ichthyocarbonate produced by the Gulf toadfish (white, $n = 15$) and the Olive flounder (gray, $n = 7$ and 8, respectively). * indicates statistically significant difference from corresponding unbleached samples ($p < 0.001$ in both cases), and ◆ indicates significant difference between bleached ichthyocarbonate samples produced by the Gulf toadfish (white hatched bar) and the Olive flounder (gray hatched bar, $p < 0.05$).

Olive flounder ($p = 0.38$), but significant differences in ichthyocarbonate dissolution rates arose after bleach-treatment ($p < 0.05$).

3.5. Dissolution Depth

Calculated initial sinking rates of ichthyocarbonate range from 10 to 100's of meters per day, with larger ichthyocarbonate sinking faster than smaller ones. Here, results are reported for particles with 0.36 and 0.91 mm diameters since these particle dimensions were previously predicted to reach depths beneath the euphotic zone (500 and 1000 m, respectively; Folkerts et al., 2024). Initial sinking rates for 0.36 mm diameter Gulf toadfish ichthyocarbonate are 12.0 and 76.9 m d^{-1} for particles 0.91 mm in diameter. Ichthyocarbonate produced by the Olive flounder has an initial sinking rate of 16.2 m d^{-1} for 0.36 mm particles, and 103.6 m d^{-1} for 0.91 mm particles. Integrating these results with measurements of dissolution rate, model results predict that natural ichthyocarbonate with diameters of 0.36 and 0.91 mm produced by both species of marine fish will completely dissolve at depths ~12–15× deeper than bleach-treated counterparts (Table 1).

4. Discussion

Here we show that organic matter coatings strongly reduce the dissolution rates of sinking ichthyocarbonate, a result which holds implications for shallow ocean alkalinity cycling and the global inorganic carbon cycle. Marine carbonate production and dissolution are fundamental processes that drive the oceanic alkalinity cycle, which in turn influence the ocean's ability to buffer changes in atmospheric CO_2 through time. To predict and/or model the response of the oceans to changing pCO_2 through time, a quantitative understanding of the amount, composition, and fate of all types of marine carbonate produced in the modern oceans is required. Despite growing appreciation of the significant quantities of carbonate produced by marine fish (Folkerts et al., 2024; Ghilardi et al., 2023; Grosell & Oehlert, 2023; Oehlert, Garza, et al., 2024; Saba et al., 2021; Walsh et al., 1991; Wilson et al., 2009), the fate of naturally excreted ichthyocarbonate is poorly understood. Recent work showed that the dissolution rate of untreated ichthyocarbonate is high compared to other biogenic carbonate minerals such as aragonitic corals; thus, marine fish play an important role in determining shallow ocean alkalinity cycling and vertical alkalinity profiles in the oceans today (Folkerts et al., 2024).

4.1. Characteristics of Ichthyocarbonate-Associated Organic Matter

Ichthyocarbonate pellets occur as single, continuously connected particles, or aggregates of smaller particles comprised of microcrystalline carbonate ("micrite") attached to each other by organic matter (Figures 1a and 2a). Under cross polarized light, strong birefringence of the micrite seen in ichthyocarbonate produced by the Gulf toadfish highlights an anisotropic ellipsoidal morphology several microns in length that is consistent with the crystallite size and morphology observed via scanning electron microscopy previously (Perry et al., 2011; Salter et al., 2017, 2019; Woosley et al., 2012). Optical petrography and microCT analyses showed that organic matter occurs within the ichthyocarbonate grain in intercrystalline spaces and as exterior organic coatings (Figures 1–3). Since crystal violet stains negatively charged biomass and gram-positive bacteria in our thin section preparation approach (Nye et al., 1972; Suosaari et al., 2022; Vitek et al., 2022), regions of the thin section that are stained purple are consistent with the previously identified

Table 1
Results of Fate Model Which Predicts the Depth of Complete Dissolution for Ichthyocarbonate of Two Diameters Produced by Two Species of Marine Fish

Treatment and species	Depth of complete dissolution (m) 0.36 mm diameter	Depth of complete dissolution (m) 0.91 mm diameter
Bleached		
Gulf toadfish	1.7	25.0
Olive flounder	3.9	59.0
Natural		
Gulf toadfish	22.0	348.0
Olive flounder	46.0	737.0

negatively charged protein-rich organic matrix associated with ichthyocarbonate (Schauer & Grosell, 2017; Schauer et al., 2016, 2018) as well as microbial cells (Walsh et al., 1991). Exterior organic matter coatings on ichthyocarbonate grains were observed both in microCT analyses and optical petrography (Figures 1–3), including large, folded organic matter excreted in close association with ichthyocarbonate (Figure 2a, white arrow; Figures 3b and 3c). Within grains of Gulf toadfish ichthyocarbonate, the organic matrix is present as a dendritic network and linear rope-like features occur at the 100-μm scale (Figures 1c, 1e, 2c, and 2e). Microbial cells may be present within the dendritic network, but dark stains preclude differentiation. Further work using higher-resolution analytical approaches like scanning electron microscopy (i.e., Perry et al., 2011; Walsh et al., 1991), would be illustrative for this species. Ellipsoidal crystallites (Figures 1d and 1f) occur within the dendritic network in toadfish ichthyocarbonate, supporting the hypothesis that the organic matrix may have provided nucleation sites for carbonate mineral precipitation within the intestine (Schauer & Grosell, 2017; Schauer et al., 2016, 2018). At the resolution of microCT analysis, our results suggest that significant proportions of ichthyocarbonate produced by the Gulf toadfish are likely organic-rich in the interior (Figure 3).

Negatively charged organic matter in ichthyocarbonate produced by the Olive flounder occurs as distinct clumps separated by unstained regions in the grain (Figure 2). Within some of the distinct clumps of organic matter, small (~5 μm) circular unstained regions may reflect gram-negative bacteria. Counterstaining with safranin (Beveridge, 2009; Coico, 2005) could confirm this hypothesis. Dense accumulations of gram positive coccoidal bacteria cells can be observed in between the clumps of organic matrix (Figure 2e, white dashed arrows) in flounder ichthyocarbonate, and individual cells occur scatted throughout the organic matrix (Figure 2d). The observation that organic matter and microbial cells occur within the interior of the ichthyocarbonate suggests they were present at the time of ichthyocarbonate formation. MicroCT analyses suggest limited occurrence of organic matter in ichthyocarbonate produced by the Olive flounder within the grains (Figure 3); however, it is important to note that the working resolution of microCT scans conducted here (~10 μm) likely integrates crystallites and organic matter within each slice. These results may suggest that the spatial relationship between crystallites and organic matter in ichthyocarbonate produced by Olive flounder occurs at finer scales than in those produced by the Gulf toadfish. Consequently, microCT analyses conducted here may underestimate organic matter volumes in the samples of ichthyocarbonate produced by Olive flounder. Ellipsoidal crystallites in ichthyocarbonate have been observed to occur at length scales <1 μm up to ~10 μm using SEM (Salter et al., 2012), suggesting the need for finer scale analytical resolution than what can be achieved with microCT analysis.

Detailed work characterizing the biochemical composition and function of the proteinaceous matrix produced by the fish was conducted previously (Schauer et al., 2016, 2018; Schauer & Grosell, 2017), but potential differences in composition in ichthyocarbonate produced by different species of fish and contributions by microbial communities to ichthyocarbonate-associated organic matter were not considered. Newer results from our geochemical analyses indicated that $\delta^{13}C_{org}$ values of ichthyocarbonate-associated organic matter were significantly different between species, whereas C/N ratios were not (Figure 4). Changes in $\delta^{13}C_{org}$ values of organic matter in ichthyocarbonate produced by different species may reflect differences in diet composition (Oehlert, Garza, et al., 2024). Similar C/N ratios suggest similar origins of organic matter in ichthyocarbonate produced by both species. Comparison with published data sets of $\delta^{13}C_{org}$ values and C/N ratios used to identify the origin of organic matter, including values for marine fish muscle (Lamb et al., 2012) and the expected ranges of bacteria from Lamb

et al. (2006), were characterized by ~5‰ higher $\delta^{13}C_{org}$ values and higher molar C/N ratios ($p < 0.01$) than organic matter associated with ichthyocarbonate produced by both species studied here (Figure 4). Using this approach, it was not possible to determine the proportional contribution of intestinal microbial communities to the organic matrix production since ranges of C/N ratios and $\delta^{13}C_{org}$ values were inconsistent with published ranges of bacterial organic matter. A more robust data set across multiple species incorporating genetic markers could provide needed insight into the role of gut microbiota in organic matrix production rate and composition.

4.2. Impacts of Organic Matter Coatings on Ichthyocarbonate Fate

Organic matter coatings on ichthyocarbonate produced by two species of fish significantly reduced the dissolution rate. Prior studies have presented conflicting interpretations of the influence of organic matter coatings on the rate of carbonate dissolution, but our study is the first to directly evaluate the role of organic matter on ichthyocarbonate dissolution. Although recent work suggests that organic coatings are likely to be associated with metabolically-influenced microenvironments that lead to increased dissolution rates (Archer, 1991; Emerson & Bender, 1981; Godoi et al., 2009; Milliman et al., 1999), earlier studies hypothesized that organic coatings may quell dissolution rates by reducing the reactive surface area of the minerals in contact with seawater (Berger, 1967; Honjo & Erez, 1978; Suess, 1970). Our results support the latter hypothesis, and show that organic matter coatings on ichthyocarbonate (Figures 1–3) significantly reduce dissolution rates of excreted ichthyocarbonate (Figure 5) with natural, untreated ichthyocarbonate dissolving 13–15× slower than bleach treated ichthyocarbonate for both species ($p < 0.05$). The observation that ichthyocarbonate dissolves faster when organic coatings are oxidized holds implications for comparison with previously published studies of ichthyocarbonate solubility. While evaluation of the solubility of bleach-treated (Woosley et al., 2012) or dissection-collected (Foran et al., 2013) ichthyocarbonates has provided important insights into their fate, recent use of natural ichthyocarbonates to estimate dissolution rates is proposed to provide a more representative understanding of the fate of ichthyocarbonates in modern oceanic conditions (Folkerts et al., 2024). For instance, our predicted depths of complete dissolution are more than an order of magnitude greater for natural ichthyocarbonate compared to bleach-treated ichthyocarbonate (Table 1), demonstrating the impact of sample pre-treatment on estimates of ichthyocarbonate fate. Importantly, these results indicate the primary role that organic coatings play in determining the role of ichthyocarbonate in the marine carbon cycle by isolating mineral crystallites from the seawater and extending their transit duration prior to complete dissolution.

Although dissolution rates of natural ichthyocarbonate were not significantly different between species ($p = 0.38$), significant differences were observed in bleached treatments between species (Figure 5). Bleached ichthyocarbonate produced by the Gulf toadfish dissolves faster (471.4 μeqv g^{-1} hr^{-1} on average) than similarly treated ichthyocarbonate produced by the Olive flounder (262 μeqv g^{-1} hr^{-1} on average, $p < 0.05$). Since the digestion efficiency using this bleach treatment was ~60% on powdered certified reference materials with high reactive surface areas, we conclude that the oxidation predominantly affected the external organic matter coatings. Thus, we infer that mineralogical differences may be explanatory, once a fraction of the organic matter coating is oxidized and crystallites are exposed. Folkerts et al. (2024) found that untreated ichthyocarbonate excreted by the Olive flounder contained significantly less Mg^{2+} than that released by the Gulf toadfish (24.5 ± 0.2 vs. 32.3 ± 0.8 mol%$MgCO_3$, respectively). Thus, the observation that bleach-treated ichthyocarbonate produced by the Gulf toadfish dissolves faster than that produced by the Olive flounder (Figure 5) is consistent with the hypothesis that biogenic HMC exhibits increasing mineral solubility with increasing mol%$MgCO_3$ (Bischoff et al., 1987; Chave et al., 1962; Morse & Mackenzie, 1990). Consequently, it appears that the organic coatings, which exert strong influence on dissolution rates, may mask any effects from mol%$MgCO_3$ content. Based on the two species studied here, it appears that once organic coatings have been removed, mol%$MgCO_3$ may be an important influence on dissolution rates as predicted.

4.3. Implications of Organic Matter Coatings on the Role of Ichthyocarbonate in the Carbonate Pump

The dissolution of soluble carbonate mineral phases is one of three principal mechanisms invoked to explain excess alkalinity above the aragonite saturation horizon (i.e., Liang et al., 2023), a characteristic that enables the surface oceans to buffer atmospheric CO_2 concentrations over sub-millennial timescales (Broecker, 1982; Revelle & Suess, 1957). Ichthyocarbonate is a quantitatively important type of metastable mineral that is produced in the oceans today (Oehlert, Garza, et al., 2024; Wilson et al., 2009), and ichthyocarbonate dissolution has been proposed as one explanation for excess normalized alkalinity above the aragonite saturation horizon

(Folkerts et al., 2024; Grosell & Oehlert, 2023; Wilson et al., 2009; Woosley et al., 2012). A prior study estimated that ichthyocarbonate dissolution could plausibly explain a quarter of excess normalized total alkalinity in the top 1,000 m of the oceans (Wilson et al., 2009). With revised median estimates of annual ichthyocarbonate production rates ~4.2× higher than before (Oehlert, Garza, et al., 2024), the dissolution of ichthyocarbonate may explain a more significant fraction of excess alkalinity above the aragonite saturation horizon than previously predicted.

Ichthyocarbonate-associated organic coatings may offer one explanation for why contradictory interpretations about the importance of marine fish contributions to the inorganic carbon cycle have been presented. Extrapolating the results of ichthyocarbonate solubility measurements (Woosley et al., 2012) as a proxy for the behavior of biogenic HMC in general, Sulpis et al. (2021) concluded that HMC dissolution is most important at shallow oceanic depths, with a globally averaged HMC saturation depth predicted to be 330 ± 210 m. However, in situ experiments conducted on coccoliths and foraminiferal calcite in the North Pacific Ocean suggested that the dissolution of more metastable minerals, such as aragonite and HMC, was not necessary to explain the observed patterns in regional shallow ocean carbonate chemistry (Subhas et al., 2022). Even correcting the estimated dissolution flux of ichthyocarbonate (0.02–0.07 mmol $CaCO_3$ m^{-2} d^{-1}; Wilson et al., 2009) by the increase in estimates of global ichthyocarbonate production (~4 but up to 9×; Oehlert, Garza, et al., 2024) may not fully explain the ~0.5 mmol m^{-2} d^{-1} estimated for this region (Subhas et al., 2022). This discrepancy may be explained by organic coatings. Slower dissolution rates resulting from intact organic coatings on ichthyocarbonate are likely more realistic in natural environments (Figure 5, Table 1), an observation consistent with modeled estimates of ichthyocarbonate fate based on measurements of untreated ichthyocarbonate size, sinking rate, and dissolution rates (Folkerts et al., 2024). In concert, these findings suggest that predicting the impact of ichthyocarbonate on the depth of the HMC saturation depth is complicated; higher global annual ichthyocarbonate production rates (Oehlert, Garza, et al., 2024) suggest there is more HMC available for dissolution than previously considered, but intact organic coatings produce slower dissolution rates (Folkerts et al., 2024; *this study*) than current solubility models predict. Nonetheless, it is clear that improved constraints on ichthyocarbonate fate are needed to fully quantify the impact of carbonate mineral dissolution on seawater carbonate chemistry, the buffering capacity of the oceans, Earth's climate, and the carbon cycle more broadly.

4.4. Implications for Ichthyocarbonate Organic Matter in the Biological Pump

Here, we have shown that organic matter coatings significantly influence the dissolution rate and fate of ichthyocarbonate, which has implications for shallow ocean alkalinity cycling and the global inorganic carbon cycle. However, we can also consider the impact of mineral dissolution rate on the vertical distribution of ichthyocarbonate-associated organic matter in the ocean. Previous analyses of total organic carbon content (TOC) indicated that ichthyocarbonate produced by three species of marine fish contains significant overall quantities of TOC (5.5%–40.4% d.w.; Oehlert, Garza, et al., 2024). Our new results indicate that this organic matter occurs both as embedded organic matter and external coatings (Figures 1–3). The fraction of mineral-embedded organic matter in ichthyocarbonate may be protected from shallow remineralization; thus, it is important to develop a quantitative understanding of the depth at which this embedded organic matter is released from the ichthyocarbonate mineral matrix. Organic matter released during ichthyocarbonate dissolution may have an important impact on vertical gradients in remineralization, energy sources for mesopelagic microbial communities, and nutrient profiles in the ocean.

4.5. Limitations

Despite recent advances (Bianchi et al., 2021; Folkerts et al., 2024; Ghilardi et al., 2023; Grosell & Oehlert, 2023; Oehlert, Garza, et al., 2024; Saba et al., 2021; Wilson et al., 2009; Woosley et al., 2012), uncertainty persists regarding the production magnitude, composition, and fate of ichthyocarbonate in the global oceans. In this study, we addressed key knowledge gaps ichthyocarbonate fate by investigating the role of organic matter coatings in reducing or enhancing dissolution rates of ichthyocarbonate produced by two species of marine fish. Limitations of our data set are the limited number of species investigated, and that dissolution rates with varying chemical and physical characteristics of seawater (i.e., aragonite saturation state, temperature, and pressure) were not evaluated. Our results may overestimate the ultimate depth of complete ichthyocarbonate dissolution, since dissolution rate is expected to increase with decreasing aragonite saturation state and temperature, and increasing pressure (i.e., Folkerts et al., 2024; Morse & Mackenzie, 1990). On the other hand, our estimates may be conservative because ichthyocarbonate is not exclusively excreted at the surface of the ocean, since much of the global fish biomass

inhabits mesopelagic water depths (Irigoien et al., 2014; Proud et al., 2017, 2018, 2019). Notably, the size, composition, and dissolution rate of ichthyocarbonate produced by mesopelagic fish species remain unknown; thus, we applied assumptions generated by studies of shallow marine fishes to conduct this modeling exercise. However, analysis of ichthyocarbonate produced by temperate species in temperature ranges as low as 10°C showed that ichthyocarbonate crystallite morphologies and mol%$MgCO_3$ were similar to those produced by subtropical reef-fishes (Salter et al., 2019), supporting extrapolations about mesopelagic ichthyocarbonate composition, at least for a first-order estimate of trends. Thus, while the estimates of ultimate dissolution depth presented here carry uncertainty arising from assumptions in the modeling approach, our results clearly demonstrate that organic matter coatings on ichthyocarbonates significantly delay complete dissolution.

4.6. Recommendations

Organic matter embedded within the particles may also indirectly exert an influence on the ichthyocarbonate dissolution rate through its role in the initial formation of ichthyocarbonate. Ichthyocarbonate produced by both species contains a significant fraction of organic matter embedded within the particles (Figures 1 and 2), suggesting the presence of organic matter when ichthyocarbonate initially forms in the intestine of the fish. The presence of this organic matter during the initial precipitation of ichthyocarbonate has been proposed to play a role in the mineralogy and ACMC content by prior investigations. Previous in vitro calcification experiments showed that varying concentrations of organic matter, especially a proteinaceous matrix, influenced the magnesium content of the crystallites that precipitated out of a solution analogous to intestinal fluid (Schauer et al., 2016). In addition, phosphate in ichthyocarbonate-associated organic matter has been proposed to be a stabilizing agent for amorphous phases, which contain high concentrations of Mg^{2+} and are even more soluble than HMC (Foran et al., 2013). Consequently, the presence of organic matter in the intestinal lumen may play a role in determining the crystallite morphology of ichthyocarbonate (i.e., ellipsoids, splayed bundles, dumbbells, Perry et al., 2011), which is known to correlate with mol%$MgCO_3$. For instance, Salter et al. (2018) documented higher Mg^{2+} contents observed in ACMC phases and ellipsoids, and lower mol%$MgCO_3$ in spheres, dumbbells, and rhombohedra. Further elucidation of the impacts of organic matrix composition on mol%$MgCO_3$ and morphology is warranted.

With respect to fate, controls on dissolution kinetics appear to be the first-order control on ichthyocarbonate fate rather than mineral solubility. Prior studies investigating the complexities of HMC solubility with varying mol%$MgCO_3$ have produced fundamental and important knowledge regarding the dissolution of metastable carbonate minerals (Bischoff et al., 1987; Mucci & Morse, 1984; Plummer & Mackenzie, 1974; Walter & Morse, 1985 Stabilities, Morse et al., 2007, among others). Importantly, such analysis of biogenic HMC pre-treated with either bleach or hydrogen peroxide to remove organic material (i.e., Bischoff, 1998; Subhas et al., 2018; Woosley et al., 2012) or synthetic HMC (i.e., Bischoff et al., 1983, 1985, 1987; Mackenzie et al., 1983; Mucci & Morse, 1983) informs mineral solubility, thermodynamic equilibrium, and the definition of K_{sp} values which are essential parameters in models of mineral stability. Building on this detailed knowledge base, our results suggest that further studies focused on the fate of untreated HMC will provide additional insight regarding the role of HMC dissolution in shallow alkalinity cycles. It is possible that suppressed dissolution rates induced by organic coatings may also apply to other metastable carbonate phases such as aragonite. For instance, early work on aragonite indicated that dissolution rates of pteropod shells collected from a sediment core dissolved at rates approximately ∼25× slower than aragonite synthesized in laboratory settings (Morse et al., 1979). Another early in situ study investigating biogenic carbonate mineral dissolution found that bleached treated biogenic carbonates dissolved faster than unbleached counterparts (Honjo & Erez, 1978), although a recent study found otherwise for coccolithophores (Subhas et al., 2018). Since coccolithophores typically have significantly lower PIC:POC ratios (Findlay et al., 2011) than ichthyocarbonate (Oehlert, Garza, et al., 2024), a minimum thickness of external organic coatings may be required to suppress dissolution rates. Thus, it is possible that organic matter coatings also play a significant role in determining the fate of other metastable carbonate minerals. Recent detailed work outlining kinetic controls on low magnesium calcite dissolution provides a useful foundation for future studies aiming to determine the impacts of pressure, organic matter, and temperature (Adkins et al., 2021; Dong et al., 2018, 2019, 2020; Liang et al., 2023; Naviaux, Subhas, Dong, et al., 2019; Naviaux, Subhas, Rollins et al., 2019; Subhas et al., 2015, 2022; Ziveri et al., 2023) on dissolution rates of biogenic HMC when organic matter coatings are kept intact.

5. Conclusions

Our integration of geochemical, petrographic, and microstructural analyses indicates that ichthyocarbonate contains significant amounts of organic matter, occurring both as exterior organic coatings and within microscale intercrystalline spaces. Intercrystalline organic matter and microbial cells suggest the presence of these organic phases during ichthyocarbonate formation, suggesting a potential role in the process of precipitation. Through the dissolution rate experiments conducted here, external organic matter coatings reduced the dissolution rate of ichthyocarbonate by up to 15×, and extended the ultimate depth of dissolution by at least 12×, revealing that ichthyocarbonate-associated organic matter plays an important role in defining the impact of ichthyocarbonate dissolution on vertical alkalinity profiles in the ocean and the global carbon cycle more broadly. Ultimately, organic matter coatings appear to be a strong determinant of ichthyocarbonate fate in the modern oceans, governing whether they dissolve and contribute to alkalinity in seawater or accumulate in sedimentary deposits in the marine environment.

Data Availability Statement

Data sets generated through this study, including dissolution rate measurements on natural and bleach-treated ichthyocarbonate, compositional analyses, and volumetric analyses conducted on microCT data sets are available as a Mendeley Dataset via: https://doi.org/10.17632/7mt9cf89ws.2 with a CC BY 4.0 License (Oehlert, Walls, et al., 2024).

Acknowledgments
We thank Grace Saba, an anonymous reviewer, and the Associate Editor for providing constructive feedback which improved this manuscript. The authors acknowledge the Stable Isotope Laboratory, including Amel Saied, Chaojin Lu, and Peter Swart for sample analyses conducted on the Costech EA and Delta V Advantage. MG is a Maytag Chair of Ichthyology. E.J.F. is supported through a Natural Sciences and Engineering Research Council of Canada Postdoctoral Fellowship. A.M.O., M.G., and S.W. acknowledge support from the National Science Foundation Chemical Oceanography Program (NSF-OCE-2319245), and A.M.O. acknowledges startup funds provided by the Rosenstiel School of Marine, Atmospheric, and Earth Science. The X-ray micro-CT imaging was made possible by the National Science Foundation under the MRI award number 1920127. Any opinions, findings, and conclusions or recommendations expressed in this material are those of the author(s) and do not necessarily reflect the views of the National Science Foundation.

References

Adkins, J. F., Naviaux, J. D., Subhas, A. V., Dong, S., & Berelson, W. M. (2021). The dissolution rate of $CaCO_3$ in the ocean. *Annual Review of Marine Science*, *13*(1), 57–80. https://doi.org/10.1146/annurev-marine-041720-092514

Archer, D. E. (1991). Equatorial Pacific calcite preservation cycles: Production or dissolution? *Paleoceanography and Paleoclimatology*, *6*(5), 561–571. https://doi.org/10.1029/91pa01630

Bar-On, Y. M., Phillips, R., & Milo, R. (2018). The biomass distribution on Earth. *Proceedings of the National Academy of Sciences of the United States of America*, *115*(25), 6506–6511. https://doi.org/10.1073/pnas.1711842115

Berger, W. G. (1967). Foraminiferal ooze: Solution at depth. *Science*, *156*(3773), 383–385. https://doi.org/10.1126/science.156.3773.383

Beveridge, T. J. (2009). Use of the gram stain in microbiology. *Biotechnic & Histochemistry*, *76*(3), 111–118. https://doi.org/10.1080/bih.76.3.111.118

Bianchi, D., Carozza, D., Galbraith, E., Guiet, J., & DeVries, T. (2021). Estimating global biomass and biogeochemical cycling of marine fish with and without fishing. *Science Advances*, *7*(41), eabd7554. https://doi.org/10.1126/sciadv.abd7554

Bischoff, W., Mackenzie, F. T., & Bischop, F. (1987). Stabilities of synthetic magnesian calcites in aqueous solution: Comparison with biogenic materials. *Geochimica et Cosmochimica Acta*, *51*(6), 1413–1423. https://doi.org/10.1016/0016-7037(87)90325-5

Bischoff, W. D. (1998). Dissolution enthalpies of magnesian calcites. *Aquatic Geochemistry*, *4*(3/4), 321–336. https://doi.org/10.1023/a:1009684214945

Bischoff, W. D., Bishop, F. C., & Mackenzie, F. T. (1983). Biogenically produced magnesian calcite; inhomogeneities in chemical and physical properties; comparison with synthetic phases. *American Mineralogist*, *68*(11–12), 1183–1188.

Bischoff, W. D., Sharma, S. K., & MacKenzie, F. T. (1985). Carbonate ion disorder in synthetic and biogenic magnesian calcites: A Raman spectral study. *American Mineralogist*, *70*(5–6), 581–589.

Brix, K. V., Wood, C. M., & Grosell, M. (2013). Measuring titratable alkalinity by single versus double endpoint titration: An evaluation in two cyprinodont species and implications for characterizing net H^+ flux in aquatic organisms. *Comparative Biochemistry and Physiology a-Molecular & Integrative Physiology*, *164*(1), 221–228. https://doi.org/10.1016/j.cbpa.2012.09.010

Broecker, W., & Peng, T. H. (1982). *Tracers in the sea*. Lamont-Doherty Geological Observatory. Columbia University.

Broecker, W. S. (1982). Glacial to interglacial changes in ocean chemistry. *Progress in Oceanography*, *11*(2), 151–197. https://doi.org/10.1016/0079-6611(82)90007-6

Chave, K., Deffeyes, K., Weyl, P., Garrels, R., & Thompson, M. (1962). Observations on the solubility of skeletal carbonates in aqueous solutions. *Science*, *137*(3523), 33–34. https://doi.org/10.1126/science.137.3523.33

Coico, R. (2005). Gram staining. *Current Protocols in Microbiology*, *00*(1), A.3C.1–A3C.2. https://doi.org/10.1002/9780471729259.mca03cs00

Coplen, T. B., Brand, W. A., Gehre, M., Gröning, M., Meijer, H. A. J., Toman, B., & Verkouteren, R. M. (2006). New guidelines for $\delta^{13}C$ measurements. *Analytical Chemistry*, *78*(7), 2439–2441. https://doi.org/10.1021/ac052027c

Corliss, B. H., & Honjo, S. (1981). Dissolution of deep-sea benthonic foraminifera. *Micropaleontology*, *27*(4), 1–9. https://doi.org/10.2307/1485191

Crowley, B. E., & Wheatley, P. V. (2014). To bleach or not to bleach? Comparing treatment methods for isolating biogenic carbonate. *Chemical Geology*, *381*, 234–242. https://doi.org/10.1016/j.chemgeo.2014.05.006

DeVries, T., & Weber, T. (2017). The export and fate of organic matter in the ocean: New constraints from combining satellite and oceanographic tracer observations. *Global Biogeochemical Cycles*, *31*(3), 535–555. https://doi.org/10.1002/2016gb005551

Dong, S., Berelson, W. M., Adkins, J. F., Rollins, N. E., Naviaux, J. D., Pirbadian, S., et al. (2020). An atomic force microscopy study of calcite dissolution in seawater. *Geochimica et Cosmochimica Acta*, *283*, 40–53. https://doi.org/10.1016/j.gca.2020.05.031

Dong, S., Berelson, W. M., Rollins, N. E., Subhas, A. V., Naviaux, J. D., Celestian, A. J., et al. (2019). Aragonite dissolution kinetics and calcite/aragonite ratios in sinking and suspended particles in the North Pacific. *Earth and Planetary Science Letters*, *515*, 1–12. https://doi.org/10.1016/j.epsl.2019.03.016

Dong, S., Subhas, A. V., Rollins, N. E., Naviaux, J. D., Adkins, J. F., & Berelson, W. M. (2018). A kinetic pressure effect on calcite dissolution in seawater. *Geochimica et Cosmochimica Acta*, *238*, 411–423. https://doi.org/10.1016/j.gca.2018.07.015

Ducklow, H. W., Steinberg, D. K., & Buesseler, K. O. (2001). Upper ocean carbon export and the biological pump. *Oceanography*, *14*(4), 50–58. https://doi.org/10.5670/oceanog.2001.06

Dunne, J. P., Toggweiler, J. R., & Hales, B. (2012). Global calcite cycling constrained by sediment preservation controls. *Global Biogeochemical Cycles*, *26*(3). https://doi.org/10.1029/2010gb003935

Emerson, S., & Bender, M. (1981). Carbon fluxes at the sediment-water interface of the deep-sea: Calcium carbonate preservation. *Journal of Marine Research*, *39*, 139–162.

Findlay, H. S., Calosi, P., & Crawfurd, K. (2011). Determinants of the PIC: POC response in the coccolithophore *Emiliania huxleyi* under future ocean acidification scenarios. *Limnology & Oceanography*, *56*(3), 1168–1178. https://doi.org/10.4319/lo.2011.56.3.1168

Folkerts, E. J., Oehlert, A. M., Heuer, R. M., Nixon, S., Stieglitz, J. D., & Grosell, M. (2024). The role of marine fish-produced carbonates in the oceanic carbon cycle is determined by size, specific gravity, and dissolution rate. *Science of the Total Environment*, *916*, 170044. https://doi.org/10.1016/j.scitotenv.2024.170044

Foran, E., Weiner, S., & Fine, M. (2013). Biogenic fish-gut calcium carbonate is a stable amorphous phase in the gilt-head seabream, *Sparus aurata*. *Scientific Reports*, *3*(1), 1700. https://doi.org/10.1038/srep01700

Ghilardi, M., Salter, M. A., Parravicini, V., Ferse, S. C. A., Rixen, T., Wild, C., et al. (2023). Temperature, species identity and morphological traits predict carbonate excretion and mineralogy in tropical reef fishes. *Nature Communications*, *14*(1), 985. https://doi.org/10.1038/s41467-023-36617-7

Glover, C. P., & Kidwell, S. M. (1993). Influence of organic matrix on the post-mortem destruction of molluscan bivalve shells. *The Journal of Geology*, *101*, 729–741.

Godoi, R. H. M., Aerts, K., Harlay, J., Kaegi, R., Chou, L., & Van Grieken, R. (2009). Organic surface coating on Coccolithophores—*Emiliania huxleyi*: Its determination and implication in the marine carbon cycle. *Microchemical Journal*, *91*(2), 266–271. https://doi.org/10.1016/j.microc.2008.12.009

Grosell, M., & Oehlert, A. M. (2023). Staying hydrated in seawater. *Physiology*, *38*(4), 1–11. https://doi.org/10.1152/physiol.00005.2023

Honjo, S., & Erez, J. (1978). Dissolution rates of calcium carbonate in the deep ocean; an in-situ experiment in the North Atlantic Ocean. *Earth and Planetary Science Letters*, *40*(2), 287–300. https://doi.org/10.1016/0012-821x(78)90099-7

Irigoien, X., Klevjer, T. A., Røstad, A., Martinez, U., Boyra, G., Acuña, J. L., et al. (2014). Large mesopelagic fishes biomass and trophic efficiency in the open ocean. *Nature Communications*, *5*(1), 3271. https://doi.org/10.1038/ncomms4271

Jennings, S., & Collingridge, K. (2015). Predicting consumer biomass, size-structure, production, catch potential, responses to fishing and associated uncertainties in the world's marine ecosystems. *PLoS One*, *10*(7), e0133794. https://doi.org/10.1371/journal.pone.0133794

Keir, R. S. (1980). The dissolution kinetics of biogenic calcium carbonates in seawater. *Geochimica et Cosmochimica Acta*, *44*(2), 241–252. https://doi.org/10.1016/0016-7037(80)90135-0

Lamb, A. L., Wilson, G. P., & Leng, M. J. (2006). A review of coastal palaeoclimate and relative sea-level reconstructions using $\delta^{13}C$ and C/N ratios in organic material. *Earth-Science Reviews*, *75*(1–4), 29–57. https://doi.org/10.1016/j.earscirev.2005.10.003

Lamb, K., Swart, P. K., & Altabet, M. A. (2012). Nitrogen and carbon isotopic systematics of the Florida reef tract. *Bulletin of Marine Science*, *88*(1), 119–146. https://doi.org/10.5343/bms.2010.1105

Liang, H., Lunstrum, A. M., Dong, S., Berelson, W. M., & John, S. G. (2023). Constraining $CaCO_3$ export and dissolution with an ocean alkalinity inverse model. *Global Biogeochemical Cycles*, *37*(2), e2022GB007535. https://doi.org/10.1029/2022gb007535

Mackenzie, F. T., Bischoff, W. D., Bishop, F. C., Loijens, M., Schoonmaker, J., & Wollast, R. (1983). Magnesian calcites: Low-temperature occurrence, solubility, and solid solution behavior. In R. J. Reeder (Ed.), *Carbonates: Mineralogy and Chemistry, Reviews in Mineralogy* (Vol. 11, pp. 97–144). Mineralogical Society of America.

Milliman, J. D., Troy, P., Balch, W., Adams, A., Li, Y. H., & Mackenzie, F. (1999). Biologically mediated dissolution of calcium carbonate above the chemical lysocline? *Deep-Sea Research I*, *46*(10), 1653–1669. https://doi.org/10.1016/s0967-0637(99)00034-5

Morse, J. W., Arvidson, R. S., & Lüttge, A. (2007). Calcium carbonate formation and dissolution. *Chemical Reviews*, *107*(2), 342–381. https://doi.org/10.1021/cr050358j

Morse, J. W., de Kanel, J., & Harris, K. (1979). Dissolution kinetics of calcium carbonate in seawater; VII, The dissolution kinetics of synthetic aragonite and pteropod tests. *American Journal of Science*, *279*(5), 488–502. https://doi.org/10.2475/ajs.279.5.488

Morse, J. W., & Mackenzie, F. T. (1990). *Geochemistry of sedimentary carbonates*. Elsevier.

Mucci, A., & Morse, J. W. (1983). The incorporation of Mg^{2+} and Sr^{2+} into calcite overgrowths: Influences of growth rate and solution composition. *Geochimica et Cosmochimica Acta*, *47*(2), 217–233. https://doi.org/10.1016/0016-7037(83)90135-7

Mucci, A., & Morse, J. W. (1984). The solubility of calcite in seawater solutions of various magnesium concentration, I_t = 0.697 m at 25°C and one atmosphere total pressure. *Geochimica et Cosmochimica Acta*, *48*(4), 815–822. https://doi.org/10.1016/0016-7037(84)90103-0

Naviaux, J. D., Subhas, A. V., Dong, S., Rollins, N. E., Liu, X., Byrne, R. H., et al. (2019). Calcite dissolution rates in seawater: Lab vs. in-situ measurements and inhibition by organic matter. *Marine Chemistry*, *215*, 103684. https://doi.org/10.1016/j.marchem.2019.103684

Naviaux, J. D., Subhas, A. V., Rollins, N. E., Dong, S., Berelson, W. M., & Adkins, J. F. (2019). Temperature dependence of calcite dissolution kinetics in seawater. *Geochimica et Cosmochimica Acta*, *246*, 363–384. https://doi.org/10.1016/j.gca.2018.11.037

Nye, O. B., Dean, D. A., & Hinds, R. W. (1972). Improved thin section techniques for fossil and recent organisms. *Journal of Paleontology*, *46*, 271–275.

Oehlert, A. M., Garza, J., Nixon, S., Frank, L., Folkerts, E. J., Stieglitz, J. D., et al. (2024). Implications of dietary carbon incorporation in fish carbonates for the global carbon cycle. *Science of the Total Environment*, *916*, 169895. https://doi.org/10.1016/j.scitotenv.2024.169895

Oehlert, A. M., & Swart, P. K. (2014). Interpreting carbonate and organic carbon isotope covariance in the sedimentary record. *Nature Communications*, *5*(1), 4672. https://doi.org/10.1038/ncomms5672

Oehlert, A. M., Swart, P. K., Eberli, G. P., Evans, S., & Frank, T. D. (2019). Multi-proxy constraints on the significance of covariant $\delta^{13}C$ values in carbonate and organic carbon during the early Mississippian. *Sedimentology*, *66*(1), 241–261. https://doi.org/10.1111/sed.12502

Oehlert, A. M., Walls, S., Arista, K., Garza, J., Folkerts, E. J., Vitek, B. E., et al. (2024). *Dataset: Composition of ichthyocarbonate and associated organic coatings*. Mendeley Data, V1. https://doi.org/10.17632/7mt9cf89ws.2

Oelkers, E. H., Golubev, S. V., Pokrovsky, O. S., & Bénézeth, P. (2011). Do organic ligands affect calcite dissolution rates? *Geochimica et Cosmochimica Acta*, *75*(7), 1799–1813. https://doi.org/10.1016/j.gca.2011.01.002

Perry, C. T., Salter, M. A., Harborne, A. R., Crowley, S. F., Jelks, H. L., & Wilson, R. W. (2011). Fish as major carbonate mud producers and missing components of the tropical carbonate factory. *Proceedings of the National Academy of Sciences of the United States of America*, *108*(10), 3865–3869. https://doi.org/10.1073/pnas.1015895108

Plummer, L. N., & Mackenzie, F. T. (1974). Predicting mineral solubility from rate data; application to the dissolution of magnesian calcites. *American Journal of Science*, *274*(1), 61–83. https://doi.org/10.2475/ajs.274.1.61

Proud, R., Cox, M. J., & Brierley, A. S. (2017). Biogeography of the global ocean's mesopelagic zone. *Current Biology*, *27*(1), 113–119. https://doi.org/10.1016/j.cub.2016.11.003

Proud, R., Cox, M. J., Le Guen, C., & Brierley, A. S. (2018). Fine-scale depth structure of pelagic communities throughout the global ocean based on acoustic sound scattering layers. *Marine Ecology Progress Series*, *598*, 35–48. https://doi.org/10.3354/meps12612

Proud, R., Handegard, N. O., Kloser, R. J., Cox, M. J., & Brierley, A. S. (2019). From siphonophores to deep scattering layers: Uncertainty ranges for the estimation of global mesopelagic fish biomass. *ICES Journal of Marine Science*, *76*(3), 718–733. https://doi.org/10.1093/icesjms/fsy037

Revelle, R., & Suess, H. E. (1957). Carbon dioxide exchange between atmosphere and ocean and the question of an increase of atmospheric CO_2 during the past decades. *Tellus*, *9*(1), 18–27. https://doi.org/10.1111/j.2153-3490.1957.tb01849.x

Saba, G. K., Burd, A. B., Dunne, J. P., Hernández-León, S., Martin, A. H., Rose, K. A., et al. (2021). Toward a better understanding of fish-based contribution to ocean carbon flux. *Limnology & Oceanography*, *66*(5), 1639–1664. https://doi.org/10.1002/lno.11709

Salter, M. A., Harborne, A. R., Perry, C. T., & Wilson, R. W. (2017). Phase heterogeneity in carbonate production by marine fish influences their roles in sediment generation and the inorganic carbon cycle. *Scientific Reports*, *7*(1), 765. https://doi.org/10.1038/s41598-017-00787-4

Salter, M. A., Perry, C. T., & Smith, A. M. (2019). Calcium carbonate production by fish in temperate marine environments. *Limnology & Oceanography*, *64*(6), 2755–2770. https://doi.org/10.1002/lno.11339

Salter, M. A., Perry, C. T., Stuart-Smith, R. D., Edgar, G. J., Wilson, R. W., & Harborne, A. R. (2018). Reef fish carbonate production assessments highlight regional variation in sedimentary significance. *Geology*, *46*(8), 699–702. https://doi.org/10.1130/g45286.1

Salter, M. A., Perry, C. T., & Wilson, R. W. (2012). Production of mud-grade carbonates by marine fish: Crystalline products and their sedimentary significance. *Sedimentology*, *59*(7), 1–27. https://doi.org/10.1111/j.1365-3091.2012.01339.x

Salter, M. A., Perry, C. T., & Wilson, R. W. (2014). Size fraction analysis of fish-derived carbonates in shallow sub-tropical marine environments and a potentially unrecognised origin for peloidal carbonates. *Sedimentary Geology*, *314*, 17–30. https://doi.org/10.1016/j.sedgeo.2014.10.005

Sarmiento, J. L., Hughes, T. M. C., Stouffer, R. J., & Manabe, S. (1998). Simulated response of the ocean carbon cycle to anthropogenic climate warming. *Letters to Nature*, *393*(6682), 245–249. https://doi.org/10.1038/30455

Schauer, K. L., Christensen, E. A. F., & Grosell, M. (2018). Comparison of the organic matrix found in intestinal $CaCO_3$ precipitates produced by several marine teleost species. *Comparative Biochemistry and Physiology a-Molecular & Integrative Physiology*, *221*, 15–23. https://doi.org/10.1016/j.cbpa.2018.03.007

Schauer, K. L., & Grosell, M. (2017). Fractionation of the Gulf toadfish intestinal precipitate organic matrix reveals potential functions of individual proteins. *Comparative Biochemistry and Physiology a-Molecular & Integrative Physiology*, *208*, 35–45. https://doi.org/10.1016/j.cbpa.2017.03.007

Schauer, K. L., LeMoine, C. M. R., Pelin, A., Corradi, N., McDonald, M. D., Warren, W. C., & Grosell, M. (2016). A proteinaceous organic matrix regulates carbonate mineral production in the marine teleost intestine. *Scientific Reports*, *6*(1), 34494. https://doi.org/10.1038/srep34494

Subhas, A. V., Dong, S., Naviaux, J. D., Rollins, N. E., Ziveri, P., Gray, W., et al. (2022). Shallow calcium carbonate cycling in the North Pacific Ocean. *Global Biogeochemical Cycles*, *36*(5). https://doi.org/10.1029/2022gb007388

Subhas, A. V., McCorkle, D. C., Quizon, A., McNichol, A., & Long, M. H. (2019). Selective preservation of coccolith calcite in Onton-Java Plateau sediments. *Paleoceanography and Paleoclimatology*, *34*(12), 2141–2157. https://doi.org/10.1029/2019pa003731

Subhas, A. V., Rollins, N. E., Berelson, W. M., Dong, S., Erez, J., & Adkins, J. F. (2015). A novel determination of calcite dissolution kinetics in seawater. *Geochimica et Cosmochimica Acta*, *170*, 51–68. https://doi.org/10.1016/j.gca.2015.08.011

Subhas, A. V., Rollins, N. E., Berelson, W. M., Erez, J., Ziveri, P., Langer, G., & Adkins, J. F. (2018). The dissolution behavior of biogenic calcites in seawater and a possible role for magnesium and organic carbon. *Marine Chemistry*, *205*, 100–112. https://doi.org/10.1016/j.marchem.2018.08.001

Suess, E. (1970). Interaction of organic compounds with calcium carbonate- I. Association phenomena and geochemical implications. *Geochimica et Cosmochimica Acta*, *34*(2), 157–168. https://doi.org/10.1016/0016-7037(70)90003-7

Sulpis, O., Jeansson, E., Dinauer, A., Lauvset, S. K., & Middelburg, J. J. (2021). Calcium carbonate dissolution patterns in the ocean. *Nature Geoscience*, *14*(6), 423–428. https://doi.org/10.1038/s41561-021-00743-y

Suosaari, E. P., Reid, R. P., Mercadier, C., Vitek, B. E., Oehlert, A. M., Stolz, J. F., et al. (2022). The microbial carbonate factory of Hamelin Pool, Shark Bay, Western Australia. *Scientific Reports*, *12*(1), 12902. https://doi.org/10.1038/s41598-022-16651-z

Vitek, B. E., Suosaari, E. P., Stolz, J. F., Oehlert, A. M., & Reid, R. P. (2022). Initial accretion in Hamelin pool microbialites: The role of *Entophysalis* in precipitation of microbial micrite. *Geosciences*, *12*(8), 304. https://doi.org/10.3390/geosciences12080304

Walsh, P., Blackwelder, P., Gill, K., Danulat, E., & Mommsen, T. (1991). Carbonate deposits in marine fish intestines: A new source of biomineralization. *Limnology & Oceanography*, *36*(6), 1227–1232. https://doi.org/10.4319/lo.1991.36.6.1227

Walter, L. M., & Morse, J. W. (1985). The dissolution kinetics of shallow marine carbonates inseawater: A laboratory study. *Geochimica et Cosmochimica Acta*, *49*(7), 1503–1513. https://doi.org/10.1016/0016-7037(85)90255-8

Wilson, R. W., Millero, F. J., Taylor, J. R., Walsh, P. J., Christensen, V., Jennings, S., & Grosell, M. (2009). Contribution of fish to the marine inorganic carbon cycle. *Science*, *323*(5912), 359–362. https://doi.org/10.1126/science.1157972

Woosley, R. J., Millero, F. J., & Grosell, M. (2012). The solubility of fish-produced high magnesium calcite in seawater. *Journal of Geophysical Research*, *117*(C4). https://doi.org/10.1029/2011jc007599

Zheng, L., & Yapa, P. D. (2000). Buoyant velocity of spherical and nonspherical bubbles/droplets. *Journal of Hydraulic Engineering*, *126*(11), 852–854. https://doi.org/10.1061/(asce)0733-9429(2000)126:11(852)

Ziveri, P., Gray, W. R., Anglada-Ortiz, G., Manno, C., Grelaud, M., Incarbona, A., et al. (2023). Pelagic calcium carbonate production and shallow dissolution in the North Pacific Ocean. *Nature Communications*, *14*(1), 805. https://doi.org/10.1038/s41467-023-36177-w